

Supporting Information

Lewis base sites of non-oxide supports boost oxygen absorption and activation over supported Pt catalysts

Jianye Liu ^a, Wenbin Chen ^a, *Taihe He* ^a, Yiwen Fang ^a, ZiYi Zhong ^{bc}, Xiaoming Wang ^a, Zhen Li ^{*a}, Yibing Song ^{*a}

^a Department of Chemistry, Shantou University, Guangdong 515063, China

^b Department of Chemistry Engineering, Guangdong Technion-Israel Institute of Technology (GTIIT), Guangdong 515063, China

^c Technion-Israel Institute of Technology (IIT), Haifa 32000, Israel

***Corresponding Authors**

E-mail addresses: lizhenlicp@stu.edu.cn (Z. Li); ybsong@stu.edu.cn (Y. Song)

Table of contents

1. Experimental section

Materials and reagents

Catalytic Activity Evaluation.

The Turnover frequency (TOF) calculation formula

2. Figure captions

Scheme S1 Schematic illustration of the preparation of Pt/CN

Scheme S2 Schematic diagram of formaldehyde catalytic oxidation

Scheme S3 The formation of pyridinic-N and pyridonic-N

Fig. S1 Energy-dispersive X-ray elemental mapping of Pt/CN-450

Fig. S2 Energy-dispersive X-ray elemental mapping of Pt/CN-550

Fig. S3 Energy-dispersive X-ray elemental mapping of Pt/CN-650

Fig. S4 X-ray diffraction (XRD) patterns of samples

Fig. S5 Fourier transform infrared (FTIR) spectra of samples

Fig. S6 O 1s spectra of the samples

Fig. S7 N₂ adsorption-desorption isotherms (a) Pt/CN-450, (b) Pt/CN-550, (c) Pt/CN-650.

3. Table

Table S1 The ratio of C to N calculated based on Elemental analyzer

Table S2 Textural properties of catalysts and TON

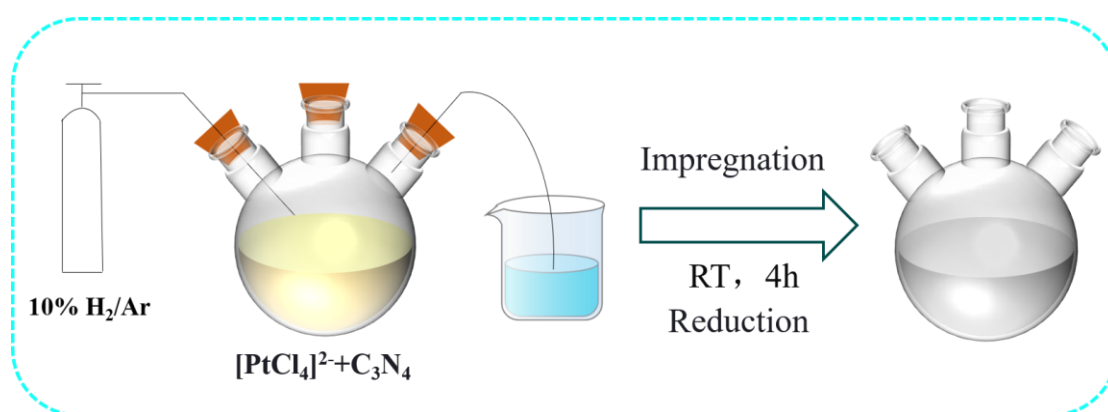
Table S3 Overview of catalytic activities in HCHO oxidation of supported Pt catalysts

EXPERIMENTAL SECTION

Materials and reagents

All of the chemicals and reagents used in this experiment were used as-received without further purification. Urea was obtained from Xilong Chemicals. Potassium tetrachloroplatinate(II) was obtained from Beijing Innochem Technology Co. Ltd. Formaldehyde standard solution (100 mg/L), Ammonium iron(III) sulfate ($\text{NH}_4\text{Fe}(\text{SO}_4)_2 \cdot 12\text{H}_2\text{O}$), 3-Methyl-2-benzothialinone ($\text{C}_6\text{H}_4\text{SN}(\text{CH}_3)\text{C}/\text{NNH}_2 \cdot \text{HCl}$) and Formaldehyde solution were procured from macklin Co. Ltd. (Shanghai).

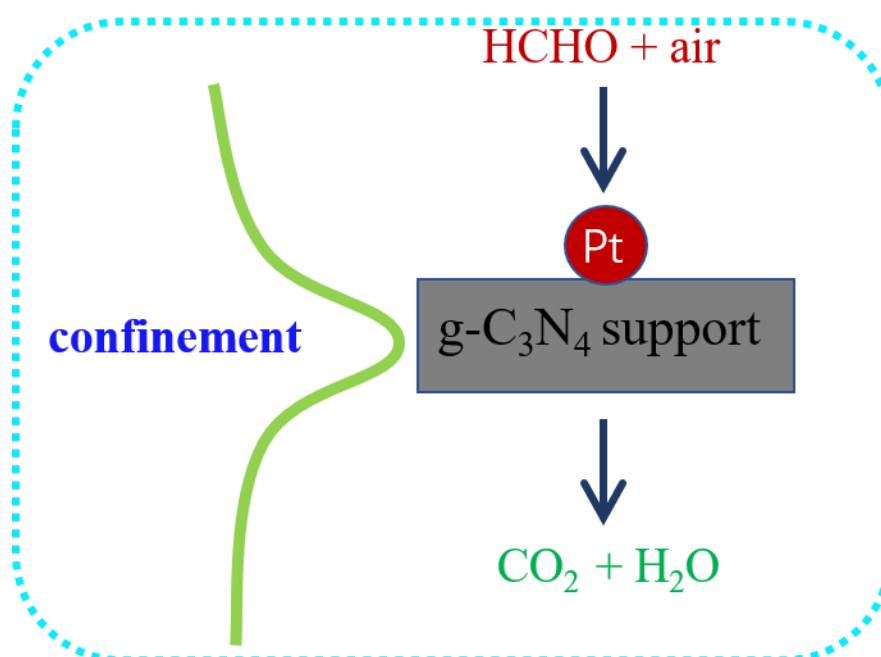
Preparation of different Pt/CN catalysts.



Scheme S1 Schematic illustration of the preparation of Pt/CN

Catalytic Activity Evaluation.

Formaldehyde in the air reacts with phenol reagent to form piperazine, which is oxidized by high iron ions in acidic solution to form blue-green compounds. The phenol spectrophotometric method for analyzing the HCHO concentration in the gaseous mixture was performed as follows: The gas stream containing trace HCHO was bubbled through 5 mL phenol reagent solution (1×10^{-4} wt%) for 30 s to collect HCHO by absorption. Then, 0.4 mL ammonium iron (III) sulfate solution (1 wt%) was added as the coloring reagent. After staying for 15 min in the dark, HCHO concentration in the gas stream was then determined by measuring light absorbance at 630 nm with a spectrophotometer.¹



Scheme S2 Schematic diagram of formaldehyde catalytic oxidation

The specific reaction rates and TOFs for HCHO oxidation at different temperatures over Pt-based catalysts were measured under differential conditions with HCHO conversion below 20% by changing the space velocity. The samples were diluted with quartz sand for the tests. The reaction rate of the catalysts was calculated by the Eq. (1):

$$(1) \gamma_{HCHO} = \frac{X_{HCHO} \cdot f_{HCHO}}{m_{cat} \cdot n}$$

Where f_{HCHO} and m_{cat} represented HCHO molar gas flow rate in $\text{mol} \cdot \text{h}^{-1}$ and the mass of catalyst in the fixed-bed, respectively; n was the loading amount of Pt.

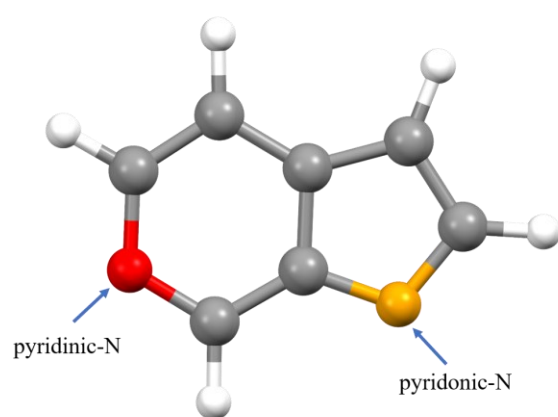
TOF was calculated based on the specific rates and Pt dispersions by the Eq. (2):

$$(2) TOF = \frac{\gamma_{HCHO} \cdot M_{Pt}}{D_{Pt}}$$

Where M_{Pt} was the molar weight of Pt and D_{Pt} represented the dispersion of Pt. TEM-derived dispersion (D_{Pt}) were obtained using the Eq. (3):²

$$(3) D_{Pt} = \left(1.483 \times \frac{(d^2)}{(d^3)} - 0.733 \times \frac{(d)}{(d^3)} + \frac{0.121}{(d^3)} \right) * 100\%$$

Where d was the average Pt particle size detected in the TEM image of the samples.



Scheme S3 The formation of pyridinic-N and pyridonic-N

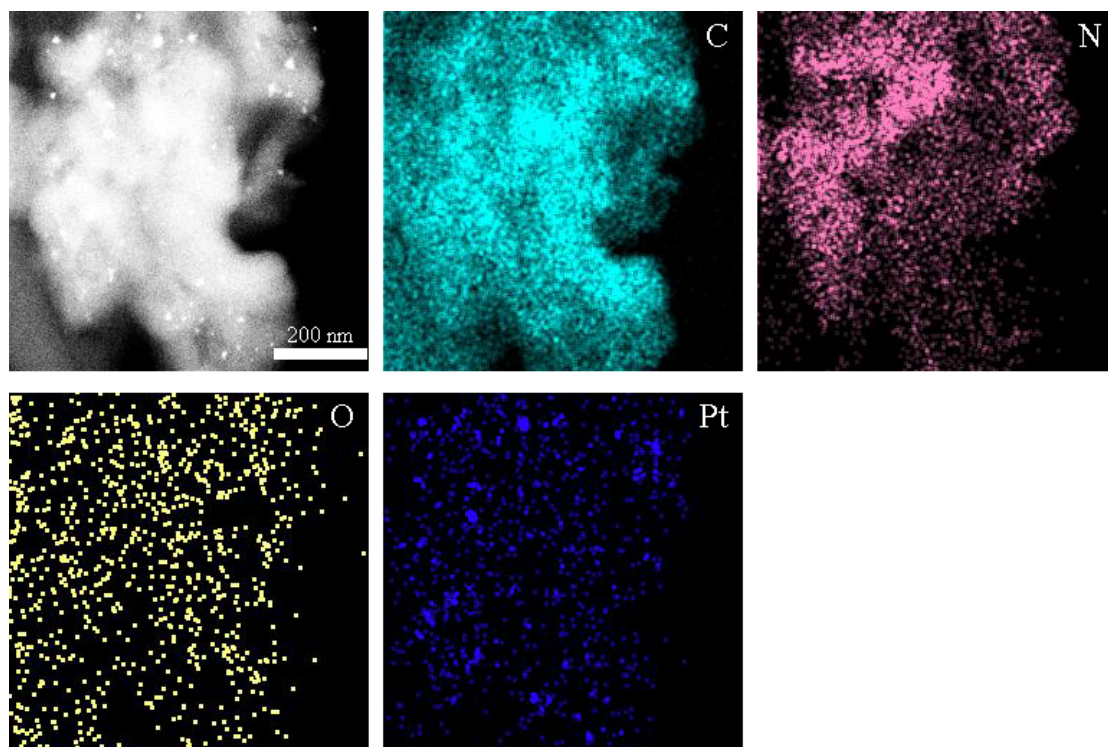


Fig. S1 Energy-dispersive X-ray elemental mapping of Pt/CN-450

Fig. S1 suggesting that carbon, nitrogen, oxygen and platinum were homogeneously distributed in Pt/CN-450.

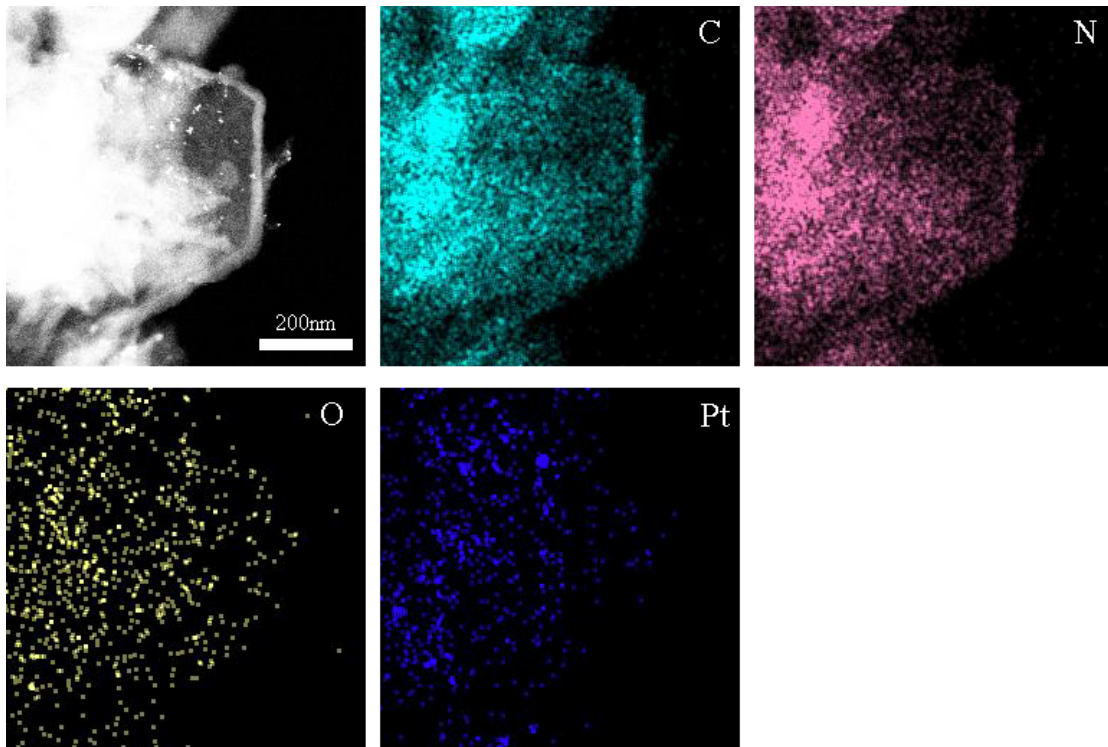


Fig. S2 Energy-dispersive X-ray elemental mapping of Pt/CN-550

Fig. S2 suggesting that carbon, nitrogen, oxygen and platinum were homogeneously distributed in Pt/CN-550.

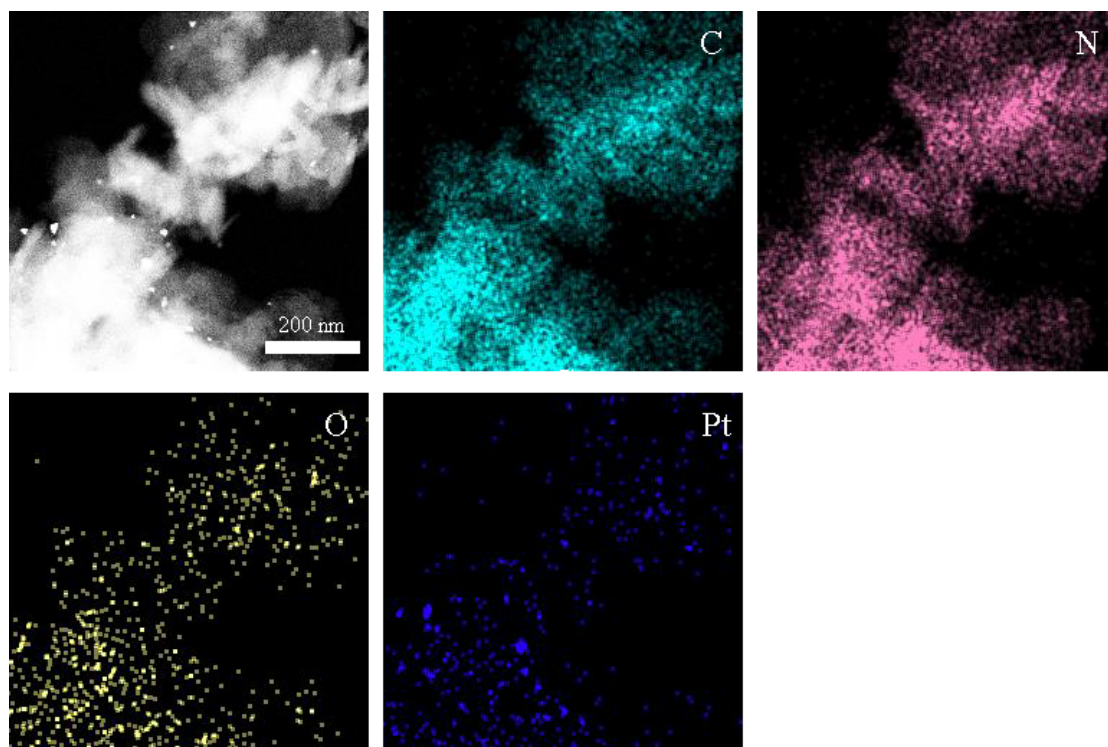


Fig. S3 Energy-dispersive X-ray elemental mapping of Pt/CN-650

Fig. S3 suggesting that carbon, nitrogen, oxygen and platinum were homogeneously distributed in Pt/CN-650.

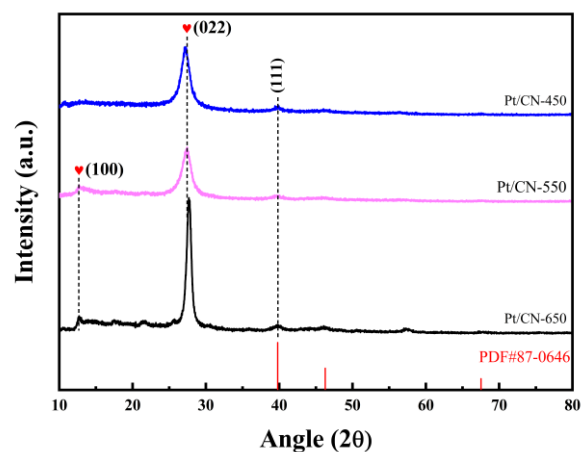


Fig. S4 X-ray diffraction (XRD) patterns of samples

The XRD patterns of the samples were showed that there were two broad peaks observed at 12.7 and 27.5° , which were ascribed to carbon nitride. There were a weak diffraction peaks of Pt species at 39.9° observed in the profiles, indicating that the main exposure of Pt species was 111 crystal plane, which was consistent with the results of HRTEM.³

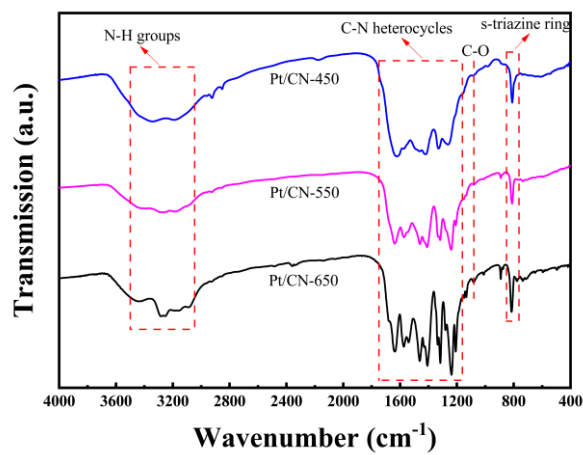


Fig. S5 Fourier transform infrared (FTIR) spectra of samples

There was little difference between the FT-IR spectra of platinum-loaded carbon nitride and carbon nitride.

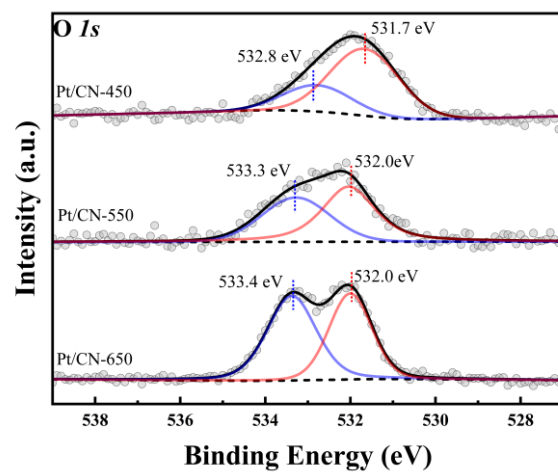


Fig. S6 O 1s spectra of the samples

In Fig. S6, the O 1s spectra were fitted to two peaks, belonging to the adsorbed water molecules (533.1 ± 0.3 eV) and C-O.^{4,5}

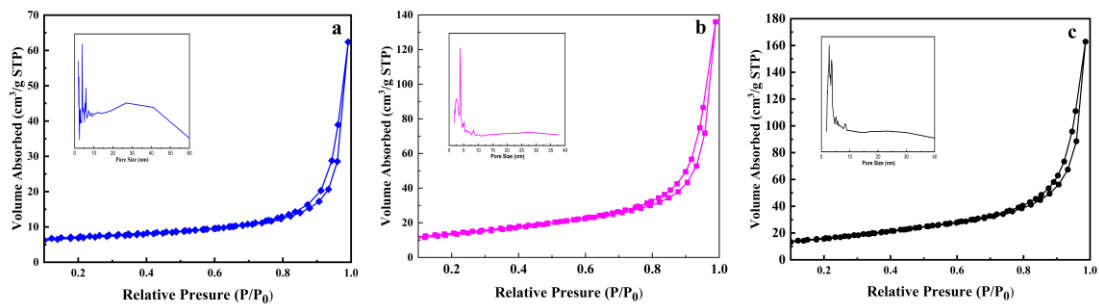


Fig. S7 N₂ adsorption-desorption isotherms (a) Pt/CN-450, (b) Pt/CN-550, (c) Pt/CN-

650.

N₂ adsorption-desorption isotherms of these samples were typical of type III with a H₃-type hysteresis loop. according to the IUPAC classification. The concave curve indicated the force of this kind of adsorption is quite weak. ⁶

Table S1 The ratio of C to N calculated based on Elemental analyzer

Sample	Element content (%)			C/N
	C	N	H	Ratio
Pt/CN-450	32.70	58.81	1.09	0.56
Pt/CN-550	34.28	60.83	0.97	0.56
Pt/CN-650	35.17	61.63	0.72	0.57

As listed in Table S1, the C/N ratio for all the samples was close, indicating that the C₆N₇ tri-s-triazines skeleton was well maintained after changing the preparation temperature of material. ⁵

Table S2 Textural properties of catalysts and TON

Sample	Surface area (m ² /g) ^a	Pore volume (cm ³ /g) ^b	Average pore diameter (nm)	TON (mol/g) ^c
Pt/CN-450	23.63	0.09	22	0.13
Pt/CN-550	49.20	0.13	10.42	0.16
Pt/CN-650	57.94	0.17	10.73	0.26

^a surface area measured by BET method.

^b pore volume and diameter determined by BJH method.

^c The number of molecules of reactants transformed on the unit active center within 30s of sampling.

Table S3 Overview of catalytic activities in HCHO oxidation of supported Pt catalysts

Catalyst	Reaction conditions	T (°C)	HCHO Conversion	Ref.
Pt/C ₃ N ₄	80 ppm HCHO; GHSV = 50000 h ⁻¹	25	100%	This work
Pt/carbon	100 ppm HCHO; GHSV = 1120 h ⁻¹	150	100%	[7]
Pt/AC	100 ppm HCHO; GHSV = 60000 h ⁻¹	80	100%	[8]
Na-Pt/AC-R	230 ppm HCHO; GHSV = 150,000 h ⁻¹	25	100%	[9]
Pt/graphene aerogel	100 ppm HCHO; GHSV = 15000 h ⁻¹	25	100%	[10]
Pt/Ni-Al LDO	100 ppm HCHO; GHSV = 6000 h ⁻¹	25	10%	[11]
Pt/birnessite	460 ppm HCHO; GHSV = 30000 h ⁻¹	20	28%	[12]
Pt/ZSM-5 zeolite	50 ppm HCHO; GHSV = 30000 h ⁻¹	30-40	95%	[13]
Pt/Al-rich Beta zeolite	80-400 ppm HCHO; GHSV = 60000 h ⁻¹	25-40	100%	[14]

References

1. J. Chen, J. Ding, H. Li, J. Sun, Z. Rui and H. Ji, *Catal. Sci. Technol.*, 2019, **9**, 3287-3294.
2. E. M. Slavinskaya, L. S. Kibis, O. A. Stonkus, D. A. Svintsitskiy, A. I. Stadnichenko, E. A. Fedorova, A. V. Romanenko, V. Marchuk, D. E. Doronkin and A. I. Boronin, *ChemCatChem.*, 2021, **13**, 313-327.
3. S. Mukerjee, S. Srinivasan, M. P. Soriaga and J. McBreen, *J. Phys. Chem.*, 1995, **99**, 4577-4589.
4. J. Li, B. Shen, Z. Hong, B. Lin, B. Gao and Y. Chen, *Chem. Commun.*, 2012, **48**, 12017–12019.
5. D. Chen, G. Zhang, M. Wang, N. Li, Q. Xu, H. Li, J. He and J. Lu, *Angew. Chem. Int. Ed.*, 2020, **60**, 6377-6381.
6. S. Yu, J. Li, Y. Zhang, M. Li, F. Dong, T. Tierui Zhang and H. Huang, *Nano Energy*, 2018, **50**, 383-392.
7. K. T. Chuang, B. Zhou and S. Tong, *Ind. Eng. Chem. Res.*, 1994, **33**, 1680.
8. W. Bao, H. Chen, H. Wang, R. Zhang, Y. Wei and L. Zheng, *ACS Appl. Nano Mater.*, 2020, **3**, 2614-2624.
9. C. Wang, Y. Li, L. Zheng, C. Zhang, Y. Wang, W. Shan, F. Liu and H. Hong, *ACS Catal.*, 2021, **11**, 456-465.
10. X. Jiang, W. Yao, J. Wang, L. Ling and W. Qiao, *Ind. Eng. Chem. Res.*, 2018, **57**, 14544–14550.
11. M. Lin, X. Yu, X. Yang, K. Li, M. Ge and J. Li, *Catal. Sci. Technol.*, 2017, **7**,

1573–1580.

12. L. Liu, H. Tian, J. He, D. Wang and Q.W. Yang, *J. Environ. Sci.*, 2012, **24**, 1117–1124.

13. H. Chen, Z. Rui, X. Wang and H. Ji, *Catal. Today*, 2015, **258**, 56–63.

14. L. Zhang, L. Chen, Y. Li, Y. Peng, F. Chen, L. Wang, C. Zhang, X. Meng, H. He and F.S. Xiao, *Appl. Catal., B.*, 2017, **219**, 200–208.